A highly modular simulation model for hybrid electric fuel cell power drive trains

S. Naylor*, V. Pickert*

**School of Electrical, Electronic and Computer Engineering, Newcastle University, UK, (e-mail: volker.pickert@ncl.ac.uk)*

Abstract: Over the last decade there has been an increasing interest on power drive train topologies for hybrid electric fuel cell vehicles. A review of previous publications revealed that little work provided direct comparisons between the topologies. This paper details the development of a simulation model that has formed the basis of an assessment of all the topologies, addressing the advantages and disadvantages of each circuit. By using a modular design concept the simulation model provided a fast method for evaluating a large variety of complex power drive train topologies from a single set of common power train components on a single vehicle chassis allowing valid conclusions to be drawn and provide the basis for future work on developing and improving existing systems and formulating new topologies.

1. INTRODUCTION

In recent computer simulation Pickert and Naylor have demonstrated that there are currently no hybrid electric fuel cell power drive train topologies that give both high performance and high efficiency. Pickert and Naylor studied more then ten different hybrid power drive trains. This paper describes for the first time the simulation tool and control algorithms used. The challenge was to design a single simulation model for power drive trains which could simulate more then 10 completely different power drive trains within a limited time period. Some of the hybrid power drive trains are shown in the Appendix of the paper. Prudent design sense suggested that instead of designing a new simulation model for each topology, designing a library of modular components and then creating each topology from these components would be the most efficient way of creating the simulation models. Not only would it ensure that common components are the same across all topologies, but also that if any changes needed to be made to any part of the model the change could be implemented across all topologies with speed and ease. Maintaining more then 10 different power drive train models for each of the topologies would quickly have become unmanageable, hard to document and cast doubt on the comparability and reliability of the simulation data.

To enable the modular design, interconnections between the different components of the drive trains were defined and standardised to ensure that a single architecture control system could control each and every topology with only minor changes of control system parameters. The control system was designed using a single control loop to ensure that the simulations could be run on a standard desktop computer in an acceptable time.

The simulation software Matlab/Simulink was chosen for the study published by Pickert and Naylor because it is a proven, industry standard package and Figure 1 shows only one example configuration for one particular power drive train.

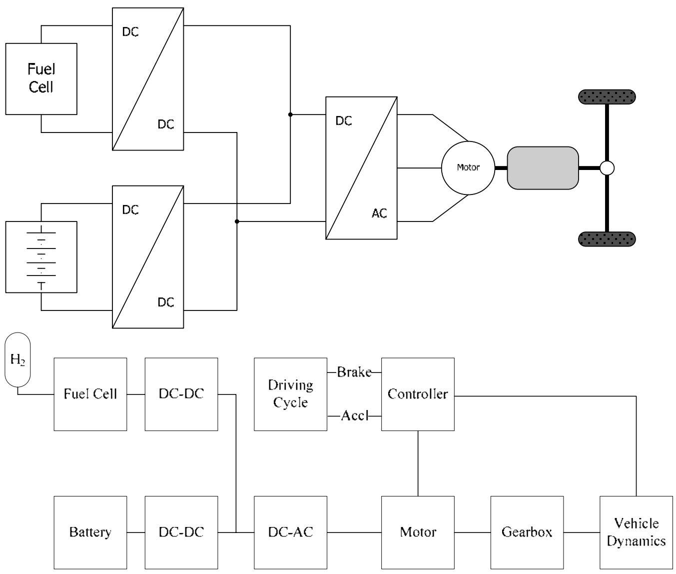

Fig. 1. Top: Topology of a hybrid electric fuel cell power drive train. Bottom: Equivalent schematic of simulation model

The paper will discuss in detail the models, and sub-models, standardisation of parameters and the implemented control algorithm. It will discuss the weaknesses and advantages of the developed simulation tool and will address common design errors.

2. THE SIMULATION TOOL

Matlab/Simulink provides a very intuitive graphical based modelling system and is a standard throughout many areas of the engineering world. It offers an ideal environment to provide a topological simulation of a fuel cell vehicle and its subsystems. The design of complex control structures is straightforward since they can be coded in script files and then inserted into simulation blocks.

The main limitation of Simulink is the way it simulates electronic devices. Native support is limited to representing a few basic electronic components and power semiconductors are only modelled as basic on-off switches ignoring the effects of turn-on or turn off times, on-state resistance, leakage currents, parasitic capacitances and temperature effects. However although all of these are relevant to the operation of the electronic power conversion systems in a fuel cell vehicle they will be common across all topologies. Simulink can therefore be used to simulate vehicles and provide valid comparison between different topologies even though it cannot model the exact behaviour of the power devices. The use of empirical data in look up table based simulation models can be used to compensate for this.

3. THE SIMULATION TOOL

All of the simulation models are based on a common vehicle chassis and drive, common power conversion elements and common power sources. The variation between topologies is predominantly in how the selected components are arranged and the control of the various elements.

By definition, choosing to design the simulation system from modular components required the different elements of the vehicle power drive train to be defined into modules. The initial grouping of components into modules was fairly intuitive but because of the way the model solves the simulation it quickly became clear that it was necessary to have clearly defined requirements of the input and output parameters that each modular block would require so as to be sure that the model could be reconfigured quickly and still run with few or no changes of control parameters and set points. Each component of the vehicle has state variables that are of no interest to the rest of the system and that can be autonomously controlled within that component in a standalone mode or by inspection of a few standard system variables. By isolating these smaller subsystems within the modules and having only a few standardised parameters such as voltage, current, torque and speed running between the modules minimised the number of interconnections and ensured that the control remained relatively simple. Once broken down into modules, the simulation system comprises of a combination of some or all of the following components:

i) 1640kg 5 door saloon vehicle chassis (includes dynamic forces and interactions), ii) 75kW (peak mechanical power) motor & inverter drive, iii) mechanical brake system, iv) 75kW fuel cell system, v) 4.5kWHr/45kW peak power battery pack, vi) bi-directional 50kW dc-dc converter, vii) uni-directional 75kW dc-dc converter, viii) controller, ix) driving cycles.

The next section will describe the main modules listed above, the theory behind the operation of each component and the input and output parameters that each module has.

4. SUB MODELS

Vehicle chassis: The vehicle chassis model takes torque from the motor and calculates the actual speed of the vehicle, considering all the forces which act on the vehicle. The chassis model is limited in that it models the straight line dynamic behaviour of the vehicle on flat surfaces and gradients. Cornering, suspension dynamics, skid behaviour, lateral forces such as roll and pitch and advanced interaction forces and transient effects are not modelled as they had little effect on the metrics of a comparative study and would complicate the model unnecessarily. The model is based on data from a European production 5-door saloon car which has a mass of 1640kg dependant upon the exact configuration of the power drive train. The mass of various components is added to the gross weight of the chassis for each topology to give a net weight for that particular drive train.

The drive train operated by calculating the angular acceleration of the vehicle based on the torque applied to the wheels by the output of the transmission, the torque applied to the vehicle by retarding forces and brakes and dividing that by the combined inertia of the vehicle, motor and transmission. The acceleration was then integrated to obtain the angular velocity of the vehicle which is then multiplied by the tire radius to obtain the linear velocity.

Controller: The primary aim of the simulation was to make a vehicle follow a driving cycle. Whilst following the driving cycle, all the components in the drive train logged various parameters to data files which were later analysed to evaluate the performance of each topology. The driving cycle replaces the role of the vehicle driver in the simulation and generates a speed demand at any given point in time during the cycle. The speed demand is the known quantity from which all other parameters in the system are derived and combined with the actual vehicle speed forms the closed loop control system which drives the car along the speed time profile of the driving cycle. Figure 2 provides an overview of this closed loop system in the context of a fuel cell battery hybrid topology.

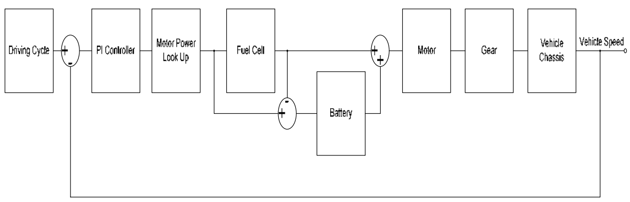

Fig. 2: Overview of the operation of the model

The following list provides a simplistic overview of how the model operates once the simulation is underway.

i) Speed demand generated by driving cycle based on a time clock signal. ii) Actual vehicle speed subtracted from speed demand to give a speed error signal. iii) PI controller generates an acceleration demand value ranging from -1 to 1 to simulate a driver following the cycle using the accelerator and brake controls as shown in Figure 10. iv) Torque demand value and actual speed passed through motor module power loss look up table. v) Electrical power loss from the motor is summed with the mechanical power to generate the total electrical traction power demand. vi) Power demand is passed to fuel cell module. vii) Fuel cell output changes to meet demand. viii) Battery pack monitors the difference between demanded power and fuel cell output power and provides the difference during the time it takes the fuel cell to respond to the demand. ix) Actual electrical output power passed to motor. x) Actual torque generated. xi) Torque passed through gearbox to vehicle chassis module. xii) Vehicle accelerates/decelerates according to the torque input. xiii) Vehicle speed decreases/increases.

This closed loop repeats until the end of the driving cycle. For the avoidance of doubt, in the case of a negative speed difference (i.e. the vehicle is required to brake) the motor module is replaced in the loop by the brake system module.

The single loop design was necessitated by the complexity, fixed step size and length of the simulation. It was found that a single PI controller with anti-windup in the outer loop allowed the simulations in a reasonable time on a standard desktop PC using a step size of 0.005s and the ODE1 (Euler) solver. The addition of further PI or PID controllers into the outer loop gave little additional beneficial control and increased the simulation time exponentially, making the simulation of multiple topologies with a range of different driving cycles impossible to complete in good time (Hauer). The controllers step response, speed error signal and vehicle speed to a demand for maximum speed from rest is shown in Figure 9 to 11.

Electric motor: The traction motor is a model based on laboratory test data from a commercially produced electric vehicle drive. The motor is a 3 phase AC induction motor capable of generating 260Nm of torque and operating at speeds of up to 10,000 rpm. The motor is driven by a 3-Phase DC-AC inverter which operates from a DC supply of 250-400V.

The model of the motor is based on two 3-dimensional look up tables. The first derives the maximum available torque at a given speed based on the input voltage by interpolating 4 torque speed curves that have been measured at 250V, 300V, 350V and 400V. The maximum available torque is an important factor in the control of the vehicle and the control system constantly monitors the DC supply voltage to the motor and the speed the motor is running at so that the maximum torque at any moment in time can be determined.

The second look up table calculates the electrical power loss in the inverter and the motor for a given speed, torque and DC supply voltage. By summing this with the mechanical power at the speed and torque the total power required by the motor is known and can be described as:

$$P_{motor} = P_{mechanical} + P_{loss}$$
$$\therefore P_{motor} = T\omega + P_{loss} \quad (1)$$

where T is the torque and ω is the mechanical frequency. Using these two look up tables the motor simulation module carries out two distinct functions.

i) Calculating the total electrical power required to achieve a given torque using speed, torque and DC voltage as lookup parameters. ii) Calculating the actual output torque for a given electrical input power using speed, power loss and DC voltage as lookup parameters.

Figure 3 and 4 show the model for motor demand power and the actual torque output. Figure 8 shows how the motor power varies with speed over the ECE driving cycle.

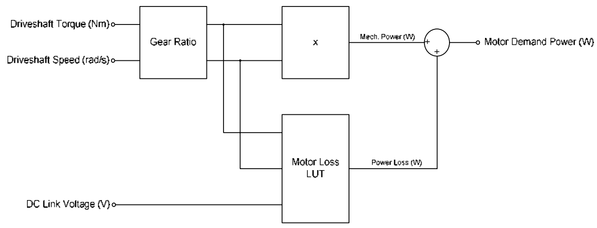

Fig. 3 Model for the motor demand power

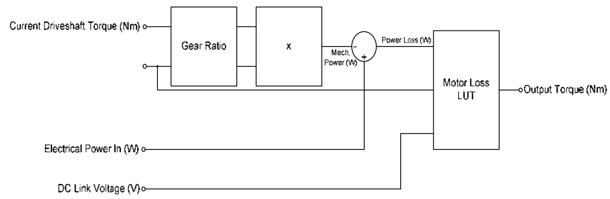

Figure 4: Model for the actual output torque

Gearbox: The gearbox used in all simulations is a fixed ratio transmission of 1:9.81. This results in a maximum available torque of 2550.6Nm and the maximum speed of the output shaft of the gearbox is 1019.37 rpm.

It is important to note that the maximum speed of the vehicle needs to be carefully monitored to prevent damaging the motor by over speeding. Since the radius of the tire is r_{tire}=0.325m and the maximum permissible speed of the motor is rpm_{max}=10,000rpm (1047.2 rad/s) the maximum speed of the vehicle can be calculated to:

$$v_{max} = 2\pi . r_{tire} \times \frac{rpm_{max}}{60}$$
$$\therefore v_{max} = 34.69ms^{-1} \quad (2)$$
$$\therefore v_{max} = 124.90kph$$

Under certain downhill road conditions this top speed could be exceeded, therefore the vehicle speed is monitored constantly and the maximum speed enforced by the control system which will actuate the vehicle brakes if necessary to protect the motor from over speeding. The efficiency of the transmission is considered as a fixed efficiency of 0.98.

Battery System Lithium ion polymer batteries (Li-Ion-P) become more and more popular as they have double the energy density of NiMH and can provide very high output power levels for short periods of time. Therefore all hybrid electric fuel cell vehicles have been simulated with Li-Ion-P batteries. The cells used in the battery pack are 4.1Ah cells with a nominal terminal voltage of 4.0V and Kokam shows the IV characteristic for each cell at the 1C (Figure 5).

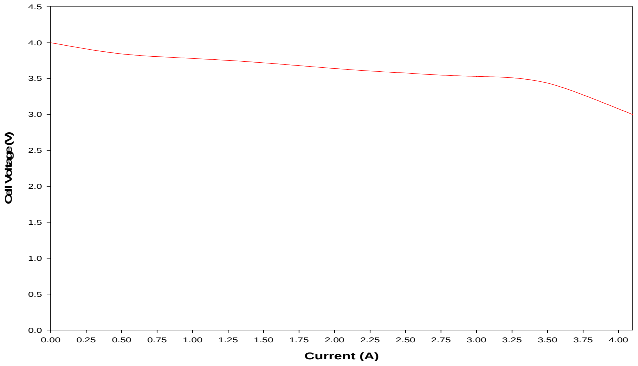

Fig. 5. Cell voltage of the Li-Ion-P battery

The maximum discharge rate of the cell is 10C (1C is defined as the rated capacity of the cell, ie the 1C rate of a 4.1Ah cell is a discharge rate of 4.1A), although this rate can only be sustained for periods of 10s at a time in order not to compromise cell life. As the discharge rate increases, the battery efficiency and terminal voltage decrease (and thus the IV characteristic changes depending on the rate of discharge). The absolute minimum terminal voltage is 2.5V though as a precaution the controller in the simulation model ensures it never drops below 3.0V. The cell is charged at 1C rate at 4.2V.

The sizing of the battery pack can be determined by two main factors, the size and the power output. Under massive transient demand, the battery pack could be expected to meet nearly 2/3 of the fuel cells rated power during the period whilst the fuel cell responds. Yet under sedate driving conditions where the transient demand rate does not exceed the fuel cells response rate the battery pack may be barely utilised at all and act as nothing more than a dead weight in the vehicle.

The battery pack was therefore constructed from 90 series sets of 4 cells in parallel. The resultant battery pack specification was thus:

Nominal terminal voltage (no-load): 369V; ii) Nominal terminal voltage (load): 270V; iii) Nominal rating: 16.4 Ah; iv) Nominal power: 4.4kW; v) Maximum power: 44.28kW; vi) Rated power: 4.4kWhr; vii) Weight: 44.1kg

Simplistically, the Matlab/Simulink model of the battery pack takes a current demand and produces a current output, pack voltage, efficiency and state of charge. The pack also takes account of negative input demands as charging currents from the fuel cell or regenerative braking, though regenerative braking is not implemented in the vehicle model.

The first step in the model is a controller which monitors the input demand. It keeps a record of the previous states of the input demand and the pack output and controls the output so that it is kept within safe limits to protect the lithium ion cells in the pack. If the current demand exceeds that which is safe for the battery at any given instant, it is limited to the safe value.

The rate of discharge is calculated and the demand is passed to a look up table which maps the rate of discharge and current to a set of IV characteristics to calculate the output voltage. The internal losses are calculated based on the manufacturers' data for the internal resistance of each cell, the cell voltage and the current drawn. The efficiency of the battery is then calculated. The diagram in Figure 6 shows the schema of the Matlab/Simulink model for the battery pack when it is being used as a power source. Charging operates in a similar way except of course the power flow is into the battery system instead of out of it.

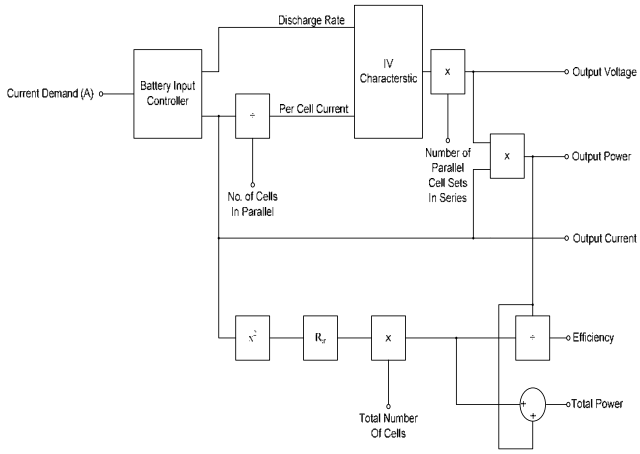

Fig. 6. Model of the battery pack

The state of charge of a battery is an indicator of how much charge the battery has left. It is expressed as a value between 0 & 1 or 0% & 100% where 0 is empty and 1 is full. It is calculated by detecting how much charge has been used at each step of the simulation, then subtracting this from the state of charge at the previous simulation step.

The exact calculation of the SOC is very difficult as it depends on many physical parameters. Various suggestions have been made to calculate the SOC and they have been published by Piller for example. For this study the following equation has been used:

$$SOC_{[i]} = SOC_{[i-1]} - \frac{P_c \times \Delta t}{3600 \times P_f} \qquad (3)$$

where P_f is the full charge power of the batter pack, P_c is the consumed power and Δt is the time of one simulation step that the power consumption is calculated over.

It is assumed that at the start of each simulation the battery SOC is 80% and it will be maintained within 40% - 80% SOC throughout the simulation as this ensures optimal battery life. In situations where power urgently is needed the SOC will be allowed to decrease below 40% but power from the battery will ultimately be cut off once the individual cell voltage reaches 3.0V to protect the cells.

Providing the simulation time step small enough (<10ms), the losses in the battery cells can be considered to be purely Ohmic and calculated from the data provided by the manufacturer. Effects such as transfer reactions and chemical diffusion can be ignored.

The current per cell can be calculated to $I_c=I_{out}/x$, where I_{out} is the battery pack output current and x is the number of cells in parallel in the pack. The battery pack power loss P_{batt_loss} is:

$$P_{batt\_loss} = (n \times x).(I_c^{\,2} \times R_{IC}) \qquad (4)$$

where R_{IC} is the internal resistance of battery cell and N is the number of series sets of parallel cells.

Temperature effects were also ignored from this study as they would have overly complicated the model and slowed down the simulation. In a practical application, the battery pack is force cooled to maintain a reasonably constant operating.

Fuel Cell System: The fuel cell model used in this study is based on empirical data from a production model 75kW (net power) direct hydrogen polymer exchange membrane fuel cell (PEMFC). Due to the vast complexity of fuel cells, modelling the electro-chemical operation of the cell within the simulation is not possible. The model is therefore based on a variety of look up tables, which characterize the operation of the fuel based on the electrical demands placed on the system.

In an actual fuel cell system the output power of the stack is controlled by changing the rate of flow of hydrogen gas through the stack. The input variable was the gas flow rate. In the model this is changed so that the input to the system is a current demand. This current demand is then fed to look up tables which contain empirical data for the fuel cell and for any given power demand determine from the input current:

i) Gas flow rate (and therefore fuel consumed), ii) Output voltage; iii) Output current; iv) Net Electrical Output Power; v) Gross Stack power; vi) Efficiency

Figure 7 shows how the system was arranged and configured in the Matlab Simulink simulation environment.

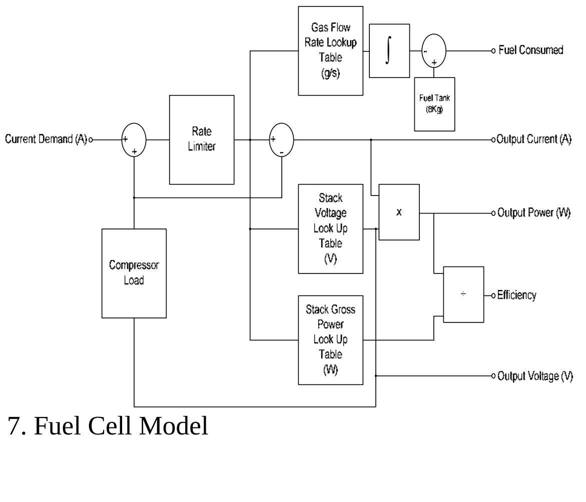

Fig. 7. Fuel Cell Model

The model includes a load for the compressor which drives the stack, this was modelled as a constant electrical load, driven by the fuel cell output. The power required to start the compressor at system start-up when the fuel cell output was zero was ignored as it was insignificant in comparison to the power consumed during driving and in any case was the same in every topology simulated and ignoring it did not adversely affect the comparisons between the performance and efficiency of the topologies.

The fuel tank is modelled as simply an 8kg store of pressurized hydrogen gas. Although in reality these tanks are very complex systems in themselves and none have yet completely eliminated hydrogen wastage through leaking, the affects of gas leakage over time were not considered in the simulation as the affect on fuel used is only detrimental when the vehicles performance is assessed over a period of days. During simulation this study only considered freshly fuelled vehicles which were driven immediately.

The response of a fuel cell to a step change in demand is inherently non-linear. Typically the time taken to change from 10% to 80% output for the fuel cell modelled is around 8 seconds, and the transient behaviour of the output is not only non-linear, but different to that had a step change of 10% to 50%. Modelling this response proved troublesome and thus it was decided that the response time would be modelled as a linear response over a period of time. This was easily implemented using a rate of change limiting function and it transpired that the net power output over the response period was not significantly different from that of the actual response, although the shape of the response was obviously quite different. Since the interest of the assessment study was power, modelling the exact response of the fuel cell to transient demand was deemed unnecessary.

Figure 8 shows how the efficiency and stack voltage of the fuel cell vary under load and illustrate the wide variation in both these parameters with the output voltage varying by over 100V across the load range and the stack efficiency ranging from 20% to 75% whilst having an average of around 60%. Variations such as these are not typical of most electrical sources and present many of the unique design problems that exist when designing fuel cell vehicle drive trains.

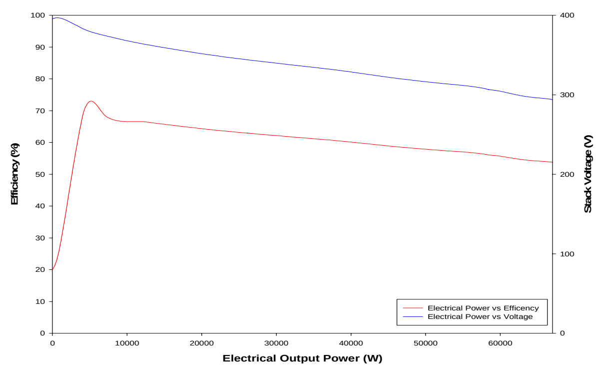

Fig. 8. Stack voltage response to load changes

5. SIMULATION RESULTS

Figures 9 to 11 show simulation results for different hybrid power drive trains. Figure 9 shows the drive power and speed profile of the topology shown in Figure 1. One can clearly see the power peaks during acceleration and the constant power during constant speed. Figure 10 shows the vehicles step response of the circuit shown in Appendix A. The car needs 17 seconds to accelerate from 0 to top speed. Figure 11 shows the PID output torque from the topology shown in Appendix B. During acceleration the output torque is positive and during braking the torque is negative. The negative torque control was set to a maximum value. Higher values are possible but will have an impact on the drivability of the vehicle.

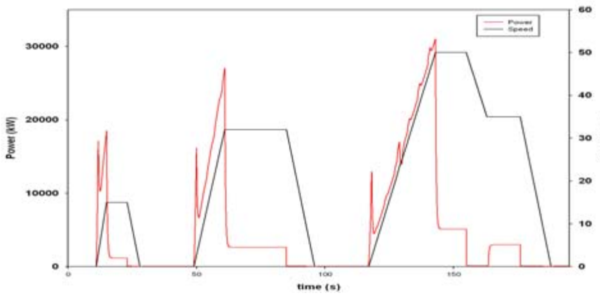

Fig. 9. Drive Power and vehicle speed for ECE Cycle

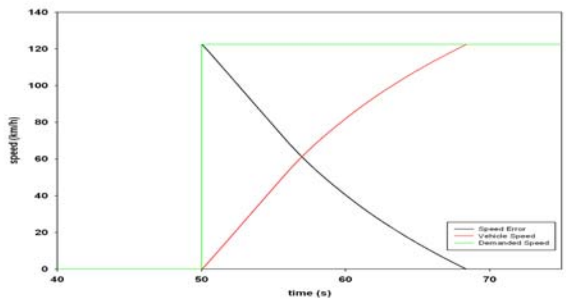

Fig. 10. Vehicle step response to full speed demand

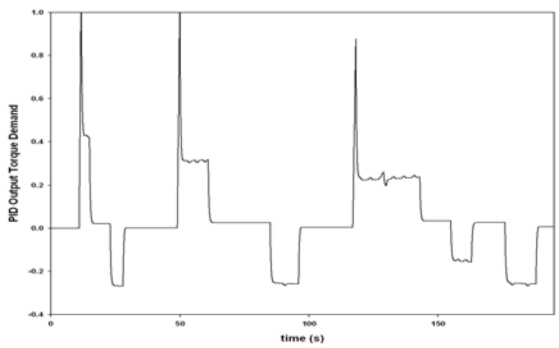

Fig. 11. PID controller response over ECE cycle

6. SUMMARY OF POWER DRIVE TRAIN COMPARISON

The simulation model presented provides a tool to compare different hybrid electric fuel cell power drive trains quickly and accurate. Results of this comparison have been published by Pickert and Naylor. It was concluded that of all power drive train variants presented, there is no single topology demonstrating fast acceleration and long range for urban, combined and highway cycles. Since the driving cycles used represent the three markets Europe, Japan and the US, it was concluded that there is no power drive train that satisfy all three markets. This consequently leads to the requirement of two power drive trains for one vehicle platform in order to satisfy all markets which is too expensive and unattractive for OEM's. Therefore research in new power drive train topologies is needed.

7. CONCLUSION

This paper has detailed the design and implementation of a modelling system that allows multiple fuel cell hybrid electric vehicle topologies to be simulated from a common set of system components and against common benchmarks. The specification of the vehicle and the design and control of its components has been discussed and the modelling of each element described. This modular system allowed topologies that had previously only been simulated and modelled in isolation, on different drive trains and against different benchmarks to be compared and contrasted based on the results from a single common vehicle chassis and drive train. Valid qualitative and quantitative conclusions about the suitability of any of the topologies for a given application were drawn and formed the basis for further simulation and hardware design work.

REFERENCES

Hauer K.H. and Moore R.M. , Fuel Cell Vehicle Simulation - Part 2: Methodology and Structure of a New Fuel Cell Simulation Tool, Fuel Cells 2003, vol. 3, pp. 95-104, 2003.

Kokam Co. Ltd.. Kokam Lithium Polymer Cell Application Manual. 2006.

Pickert V, Naylor S. Overview of Power Drive Trains for Hybrid Fuel Cell Electric Vehicles. EET-2007 European Ele-Drive Conference Brussels, Belgium, May 30 – June 01, 2007.

Pickert V, Naylor S. A review of power drive trains for hybrid fuel cell electric vehicles (HFCEV). 3rd IET Conference on Automotive Electronics, Warwick, 28-29 June 2007.

Piller S., Perrin M., and Jossen A. , Methods for state-of-charge determination and their applications, Journal of Power Sources, vol. 96, pp. 113-120, 2001.

APPENDIX

The following two figures show a selection of fuel cell topologies presented by Pickert and Naylor.